Journal of Solid State Chemistry 183 (2010) 1615–1619

Contents lists available at ScienceDirect

Journal of Solid State Chemistry

journal homepage: www.elsevier.com/locate/jssc

Coordination polymer based on cyano: Synthesis, crystal structure, and fluorescence

Zhen-Lan Fang, Jian-Gang He, Qiang Ju, Xiao-Yuan Wu, Can-Zhong Lu *

State Key Laboratory of Structural Chemistry, Fujian Institute of Research on the Structure of Matter, the Chinese Academy of Sciences, Fuzhou, Fujian 350002, PR China

ARTICLE INFO

Article history:
Received 18 March 2010
Received in revised form
2 May 2010
Accepted 9 May 2010
Available online 2 June 2010

Keywords:
Cyano
Coordination polymer
Network
Fluorescence
DFT calculation

ABSTRACT

One novel 2-D polythreading framework named as $[Cu_3(CN)_3(NH_3)]$ (**1**), was obtained through the self-assembling of CuCN under hydrothermal reaction. It is remarkable that there is a 26-membered $[Cu_{10}(CN)_8]$ decanuclear metallamacrocycle with the effective size of ca. 16.8×6.83 Å^2 along the *a*-axis. These 2-D layers stack in an $\cdots$ABAB$\cdots$ staggered fashion, with the lateral $\{(CN)Cu_3(NH_3)\}$ moieties of each layer inserting into the voids of the decanuclear metallamacrocycles from two adjacent layers. Optical diffuse reflectance spectrum and the result of DFT calculation reveal that **1** is potential direct semiconducting material. In the solid state at room temperature, **1** shows bright yellow fluorescence under ultraviolet light illumination. Its emissive excited state is primarily attributed to the LMCT, LLCT and ^{3}[MMLCT] excited state, based on the result of DFPT calculation.

1. Introduction

For several decades, metal coordination polymers have drawn considerable attentions not only for their intriguing architectures but also for potential applications in the fields of catalysis, molecular-based magnets, electrical conductivity, zeolite-like materials, etc. [1,2]. Among these metal coordination polymers, copper cyanide systems have received special interests due to their fascinating structural frameworks, superior physical and chemical properties, and potential applications in many fields [3–6]. In this system, the cyanide group is a versatile ligand that can act as a mono-dentate ligand as well as a μ_2-, μ_3-, or μ_4-bridging multi-dentate ligand, while the copper atom has versatile coordination properties and commonly adopts two-, three-, four-, five-, or six-coordination to form diverse geometries. Strong bridging tendency of the cyanide group often assists the attainment of suitable architecture for extended luminescent interactions. Therefore, the self-assembling of copper cyanide can generate long-lived and highly efficient luminescent materials with variable structures, which sometimes exhibit intriguing topological architectures [7].

Unfortunately, up to now, the research of (cyano)cuprates luminescence is restricted in the solution state due to the difficulty of preparing their pure crystalline samples. As a part of extensive study of luminescent metal-organic networks based on CuCN [8,9] herein, we report the synthesis, crystal structure, and optical absorption spectra as well as the long-lived and efficient solid-state luminescent properties of a novel type of copper(I) cyanide complex in detail for the first time.

2. Experimental

2.1. Materials and general methods

The bridging ligand L_1 [L_1=2,5-bis(4-cyanophenyl)-1,3,4-oxadiazole] (Scheme 1) was synthesized according to reported literature procedure [10]. Other chemicals were obtained from commercial sources and used without further purification. The IR spectra (KBr pellets) were recorded on a Magna 750 FT-IR spectrophotometer in the range $400-4000\ cm^{-1}$. C, H, and N elemental analyses were determined on an EA1110 CHNS-0 CE element analyzer. Powder X-ray diffraction data were recorded on a PANaytical X'pert pro X-ray diffractometer with graphite-monochromatized Cu*K*α radiation (λ=1.542 Å). Thermal stability studies were carried out on a NETSCHZ STA 449C thermoanalyzer under N_2 ($30-1200\ ^\circ C$ range) at a heating rate of $10\ ^\circ C\ min^{-1}$. Fluorescence spectra were measured with an Edinburgh Analytical instrument FLS920.

2.2. Synthesis of $[Cu_3(CN)_3(NH_3)]_n$ (**1**)

A mixture containing CuCN (200.0 mg, 0.42 mmol), L_1 (40.0 mg, 0.13 mmol), ammonia (25%, 1 ml) and deionized water

* Corresponding author.
E-mail addresses: czlu@fjirsm.ac.cn, czlu@ma.fjirsm.ac.cn (C.-Z. Lu).

0022-4596/$ - see front matter © 2010 Elsevier Inc. All rights reserved.
doi:10.1016/j.jssc.2010.05.011

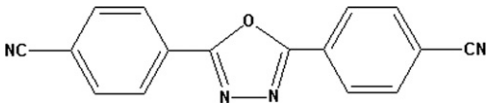

Scheme 1. The bridging ligand L_1 of the reaction.

Table 1
Crystal data and structure refinement results for **1**.

Empirical formula	$C_3H_3Cu_3N_4$
Formula weight	285.71
Cryst. syst.	Monoclinic
Space group	*C*2/*c*
Z	8
a (Å)	19.093(13)
b (Å)	6.805(4)
c (Å)	13.224(17)
α (deg)	90.00
β (deg)	125.670(7)
γ (deg)	90.00
V (Å^3)	1396(2)
ρ_{calcd} (g/cm^3)	2.719
μ (mm^{-1})	8.972
GOF	1.008
R_1 ($I>2\sigma(I)$)[a]	0.0295
wR_2 (all data)[b]	0.0823

[a] $R_1=\Sigma\|F_o|-|F_c\|/\Sigma|F_o|$.
[b] $wR_2=\{\Sigma[w(F_o^2-F_c^2)^2/\Sigma[w(F_o^2)^2]]^{1/2}$.

(14 ml), was placed in a Parr Teflon-lined stainless steel vessel (20 ml) under autogenous pressure, and stirred at room temperature for 5 h, which was then heated at 180 °C for 72 h, followed by slowly cooling to room temperature at a rate of 3 °C h^{-1}. Yellow block crystals of the product were collected, washed with H_2O, and air-dried. The yield of final product was calculated to be 52.5% based on CuCN. Anal. Calc. for $C_3H_3Cu_3N_4$: C, 12.60; H, 1.05; N, 19.60%. Found: C, 12.46; H, 1.09; N, 19.09%. FT-IR (cm^{-1}): 3345(m), 3275(m), 3176(w), 2135(s), 2095(s), 1600(m), 1242(s), 638(s).

2.3. Single-crystal structure determination.

The single crystal of **1** in the present work was mounted on a glass fiber for the X-ray diffraction analysis. Data sets were collected on a Rigaku AFC7R equipped with a graphite-monochromated MoKR radiation ($\lambda=0.71073$ Å) from a rotating anode generator at 293 K. Intensities were corrected for LP factors and empirical absorption using the ψ scan technique. The structure was solved by direct methods and refined on F^2 with full-matrix least-squares techniques using Siemens *SHELXTL* version 5 package of crystallographic software [11]. For **1**, the bridging cyanide group indicated disorder with respect to the C and N termini; this disorder was treated by adopting 50% C and N occupancies at those sites. The disordered C/N positions are labeled as CN. All nonhydrogen atoms were refined anistropically. Positions of the hydrogen atoms attached to nitrogen atom were fixed at their ideal positions. Crystal data as well as details of data collection and refinement for complex **1** are summarized in Table 1. The selected interatomic distances and bond angles are given in Table 2. CCDC-768909 (**1**) contains the supplementary crystallographic data for this paper. Copy of this data can be obtained free of charge from The Cambridge Crystallographic Data Center via www.ccdc.cam.ac.uk/datarequest/cif.

Table 2
Selected bond lengths (Å) and angles (deg) for **1**.

Cu(1)–N(6)	1.945(3)	Cu(1)–Cu(1)#1	2.6300(16)
Cu(1)–N(1)	1.965(3)	Cu(2)–N(5)	1.855(4)
Cu(1)–N(3)	1.976(4)	Cu(2)–C(4)	1.877(4)
Cu(1)–C(1)#1	2.396(3)	Cu(3)–C(2)	1.843(3)
Cu(1)–N(1)#1	2.396(3)	Cu(3)–N(7)	1.892(3)
N(6)–Cu(1)–N(1)	126.13(13)	N(3)–Cu(1)–C(1)#1	105.64(12)
N(6)–Cu(1)–N(3)	110.38(11)	N(6)–Cu(1)–N(1)#1	95.49(11)
N(1)–Cu(1)–N(3)	109.80(12)	N(1)–Cu(1)–N(1)#1	106.56(12)
N(6)–Cu(1)–C(1)#1	95.49(11)	N(3)–Cu(1)–N(1)#1	105.64(12)
N(1)–Cu(1)–C(1)#1	106.56(12)	C(1)#1–Cu(1)–N(1)#1	0.00(12)
N(6)–Cu(1)–Cu(1)#1	121.84(10)	N(5)–Cu(2)–C(4)	166.10(16)
N(1)–Cu(1)–Cu(1)#1	60.83(10)	C(1)#1–Cu(1)–Cu(1)#1	45.73(7)
N(3)–Cu(1)–Cu(1)#1	119.91(9)	N(1)#1–Cu(1)–Cu(1)#1	45.73(7)

Symmetry transformations used to generate equivalent atoms: **1**: #1 $-x+1/2$, $-y+1/2$, $-z$; #2 $-x+1$, y, $-z+3/2$; #3 $-x+1/2$, $-y+3/2$, $-z$.

2.4. Computational descriptions

The crystallographic data of **1** determined by X-ray was used to calculate its electronic band structure and the orbital plots. The density functional theory (DFT) calculations [12–15] were performed on **1** by using CASTEP code [16]. The total energy was calculated within the framework of the PW91 generalized gradient approximation [17]. The interactions between the ionic cores and the electrons were described by the norm-conserving pseudopotentials [18]. We chose an energy cutoff of the plane-wave of 550 eV and a $4\times2\times2$ Monkhorst-Pack *k*-point grid for **1**. For the calculations of the orbital plots using DMOL3 [19], we have used generalized gradient approximation functional in the manner suggested by PW91, and double numerical plus *d*-functions basis set.

3. Results and discussion

3.1. Synthesis

1 was synthesized under hydrothermal condition. These yellow crystalline solid is stable in air and insoluble in water or common organic solvents such as chloroform, ethyl acetate, ethanol, and acetone. In this work, CuCN was used as the metal source, and L_1 was selected as the bent bridging ligand. In addition, ammonia (25%, 1 ml) was used as the starting material to increase the pH value of the reaction mixture to further promote the reaction. Unfortunately, our efforts failed and only the CuCN complex was obtained in the reaction mixture, which revealed that the self-assembling of copper cyanide may have a greater tendency than the coordination between Cu ion and L_1. We have attempted to apply other available metal salts instead of CuCN in the synthesis process; however, the bridging ligand L_1 does still not incorporate in the metal-organic frameworks. Moreover, the attempt to synthesize this luminescent material **1** in the absence of L_1 has failed. Therefore, L_1 maybe is difficult to coordinate to metal centers, but play an important role of template under this reaction conditions.

3.2. Infrared spectroscopy

Infrared analysis of **1** (Fig. S1) reveals the expected intense cyanide stretching bands occurring in the 2135(s) and 2095(s), which is typical for bridging cyanide groups and higher than that of terminal cyanide ion (approx. 2050 cm^{-1}) [20]. The two absorptions for bridging cyanide groups indicate the existence

of two types of cyanide groups with μ_2 and μ_3-bridging modes. Sharp and moderately weak infrared absorptions in the 3345(m), 3275(m), 3176(w) cm^{-1} region reveal the existence of the terminal NH_3 group. These facts are all consistent with the simple structure.

3.3. Structure description

For **1**, the symmetry-related C and N atoms of cyanide are disordered, and there are three unique Cu(I) ions and cyanide groups as well as one NH_3 in the asymmetric unit (Fig. 1). The four-coordinated Cu1 atom is in a tetrahedral environment consisting of two μ_3-cyanide N(C)1 atoms, one μ-cyanide C(N)6 atom, and one μ-cyanide C(N)2 atom. The two-coordinated Cu2 is linearly connected by two cyanide N(C)4 and N(C)5 atoms to form a subunit of $[Cu_2(CN)_3]$ with the N–Cu–N bond angle of 166.097(154)°. However, the two-coordinated Cu3 is also linearly connected by one μ_3-cyanide N(C)1 atom and one N atom from ammonia, which was confirmed by IR spectrum and element analysis, with the N–Cu–N bond angle to be 174.524(164)°. The [Cu1Cu3CN(NH_3)] moieties are bridged by [CN–Cu2–CN–Cu2–CN] units to form 1-D $[Cu_6(CN)_5(NH_3)]_2$] ribbons extending along the *C*-axis (Fig. 2a). The 1-D ribbons further bridged by cyanide to extend to 2-d (4, 4) grids, resulting in the formation of fused 26-membered $[Cu_{10}(CN)_8]$ decanuclear metallamacrocycle with the effective large size of ca. 16.8 × 6.83 $Å^2$ along the *a*-axis (Fig. 2b). The Cu–Cu separation in the $[Cu1]_2$ dimer is 2.6300(15) Å, which is much shorter than the sum of van der Waals radii for copper (2.8 Å) [21], suggesting significant copper–copper interactions. Such metal–metal bonding (sometimes supported by cyano-bridging) is fairly common in these materials.

Interestingly, investigation of the crystal packing shows that these 2-D grids stack in an ABAB staggered fashion along *a*-axis to form one novel polythreading architecture (Fig. 2c and d), with the lateral {(CN)Cu3(NH_3)} moieties of each layer inserting into the voids of the decanuclear metallamacrocycles from the two adjacent layers. Analogous examples have been reported by other research groups very recently [22–24].

3.4. Luminescence property

Optical diffuse reflectance spectrum of **1** reveals the presence of the optical gap of 2.41 eV (Fig. 3). The spectrum has an intense absorption band centered at ~344 nm, which can be ascribed to intra-ligand $\pi-\pi^*$ transition. In the solid state at room temperature, **1** shows bright yellow fluorescence under ultraviolet light

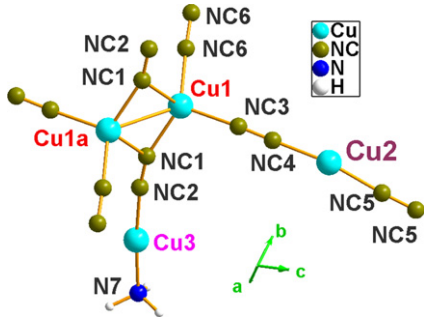

Fig. 1. Perspective view of coordination environments of Cu centers with atom labeling in **1** (atoms from the disordered C and N bridging groups are labeled as CN).

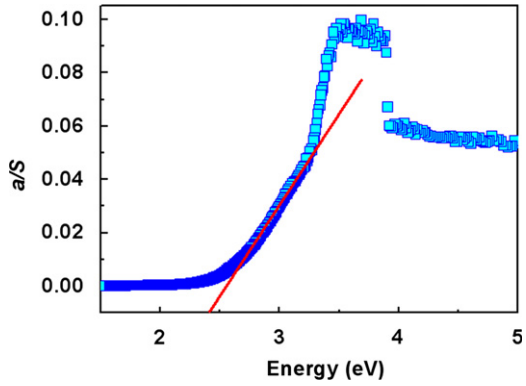

Fig. 3. Optical absorption spectra of **1**.

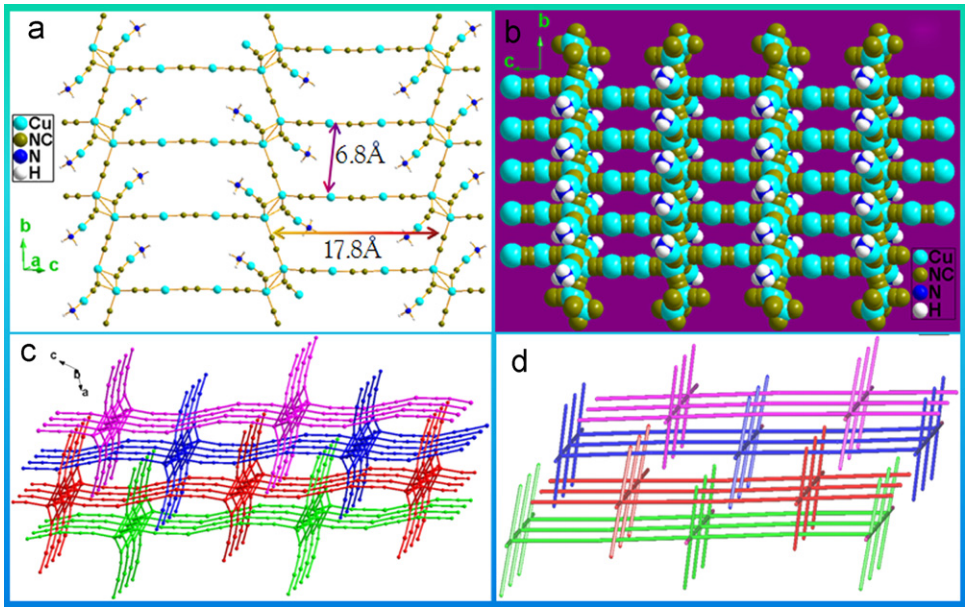

Fig. 2. (a) The related decanuclear metallamacrocycle defines the cavities of 17.8 × 6.8 Å occupied by the [Cu(CN)] moieties from the adjacent layer. (b) Space-filling views of decanuclear metallamacrocycle of the 2-D fluctuant sheet in **1**. (c) An illustration showing the polythreading fashion of the layers (indicated by different colors) in **1**. (d) The topos view of the packing diagram of the 2D networks.

illumination (Fig. 4) with a strong emission band peaked at 544 nm upon photo excitation at 344 nm. The emission at 544 nm for **1** may be assigned to metal-to-ligand charge transfer (MLCT) where the electron is transferred from the copper-(I) center to the unoccupied $\pi*$ orbitals of cyanide ligand according to the literature [25–29]. The distance of Cu1a–Cu1 [2.63 (15)] is substantially shorter than the sum of the van der Waals radii (2.80 Å,) of Cu^{I} centers [21], as a result, the metal-centered transitions ^{3}[MC] of the type $3d^{10}\rightarrow 3d^{9}4s$ and $3d^{10}\rightarrow 3d^{9}4p$ on the copper(I) center [28,30–32] or metal–metal bond to ligand charge transfer ^{3}[MMLCT] excited state may occur.

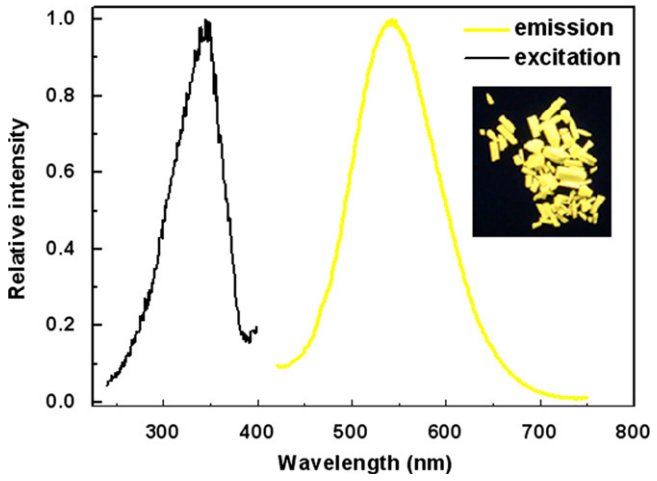

Fig. 4. Solid-state electronic emission spectra of **1** at room temperature (inset: Luminescence of **1** under ultraviolet light illumination).

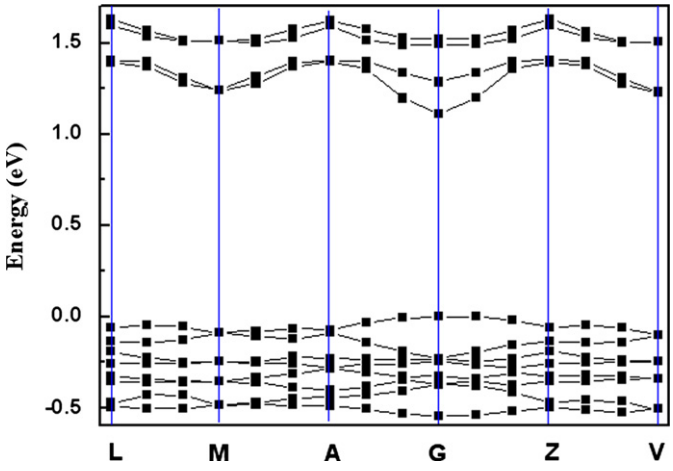

Fig. 5. Band structure of **1** calculated using DFPT within generalized gradient approximation.

The lifetime data of the emission can be well fitted by tri-exponential decay (correlation constants >0.96) with long multicomponent fluorescent lifetimes ($\tau_1=4.47$ μs, 36.37%, $\tau_2=79.33$ μs, 30.29%, and $\tau_3=1.08$ μs, 33.34%), revealing phosphorescence characteristic of the emission. A better insight of the nature of luminescence property can be achieved by the DFT calculations [12–15], which were performed by using CASTEP code [16,33]. Band structure of **1** calculated by using DFPT within generalized gradient approximation gives a band gap of 1.12 eV (Fig. 5), which is smaller than a direct optical gap of 2.39 eV obtained through UV–Vis diffuse reflective spectrum (Fig. 4). The reason for such situation is that the GGA cannot accurately describe the eigenvalues of the electronic states, which causes quantitative underestimation of band gaps [34]. These results indicate that HOMO is mostly composed of *d* orbitals of Cu^{I} and π orbitals of cyanide groups, while for LUMO, it mainly consists of *d* orbitals of Cu^{I} and π^* orbitals of cyanide groups (Fig. 6). Therefore, these results predict that the emissive excited state of **1** is primarily attributed to the LMCT plus ^{3}[LLCT] and ^{3}[MMLCT] state.

3.5. Thermogravimetric analysis (TGA) and XRPD

1 was characterized via X-ray powder diffraction (XRPD) (Fig. S2). The XRPD pattern measured for the as-synthesized samples was in good agreement with the XRPD pattern simulated from the single-crystal X-ray data. The thermal stability of **1** was investigated on crystalline samples under nitrogen atmosphere from 30 to 1200 °C. The TG curve shows (Fig. 7) that the framework was stable up to 106 °C, and had a first weight loss of 6.5% from 106 to 265 °C, corresponding to the release of one NH_3 molecule (calcd. 7.2%). No weight loss was observed from 265 to 510 °C, and a framework of

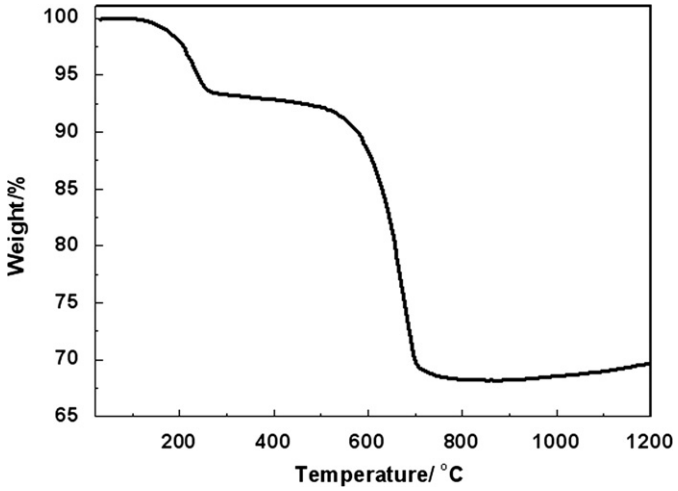

Fig. 7. TGA profiles for **1**.

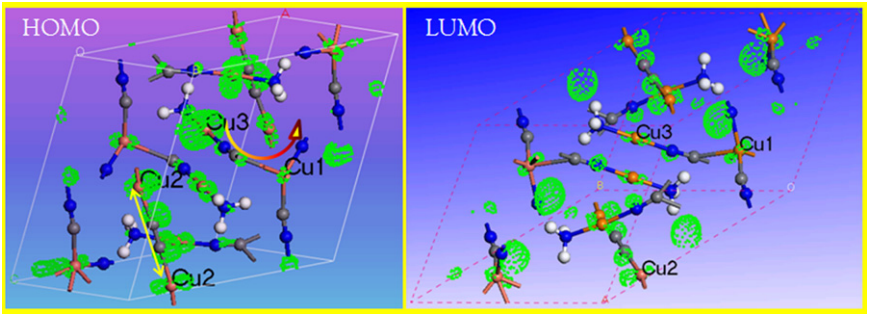

Fig. 6. Electron-density distribution of the lowest unoccupied and highest occupied frontier orbitals of **1**.

$Cu_3(CN)_3$ remained. However, the $Cu_3(CN)_3$ framework decomposed in the temperature range from 510 to 710 °C and Cu was the final product. This conclusion is supported by the percentage of the residues (68.21%), which is in accordance with the expected value (67.13%).

Above result indicates that **1** is stable for further potential applications as semiconductor or high efficient solid-state luminescent material.

4. Conclusions

In conclusion, one novel intense and long-lived luminescent material **1** with 2-D polythreading framework has been successfully synthesized through the self-assemble of CuCN under hydrothermal reaction. It is interesting that there is a fused 26-membered $[Cu_{10}(CN)_8]$ decanuclear metallamacrocycle with the effective size of ca. 16.8×6.83 Å^2 along the *a*-axis. These 2-D aggregations stack in a staggered fashion, with the lateral $\{(CN)Cu3(NH_3)\}$ components of each layer penetrating into the voids of the metallamacrocycles coming from two adjacent layers. Optical diffuse reflectance spectrum and the result of DFT calculation reveal that **1** belongs to potential semiconducting material.

Acknowledgments

This work was supported by the 973 key program of the MOST (2006CB932904, 2007CB815304, and 2010CB933501), the National Natural Science Foundation of China (20873150, 20821061, 20973173, and 50772113), the Chinese Academy of Sciences (KJCX2-YW-M05 and 319).

Appendix A. Supporting information

Supplementary data associated with this article can be found in the online version at doi:10.1016/j.jssc.2010.05.011.

References

[1] M. Verdaguer, A. Bleuzen, V. Marvaud, J. Vaissermann, M. Seuleiman, C. Desplanches, A. Scuiller, C. Train, R. Garde, G. Gelly, C. Lomenech, I. Rosenman, P. Veillet, C. Cartier, F. Villain, Coord. Chem. Rev. 192 (1999) 1023–1047.
[2] M. Ohba, H. Okawa, Coord. Chem. Rev. 198 (2000) 313–328.
[3] T. Korzeniak, K. Stadnicka, R. Pelka, M. Balanda, K. Tomala, K. Kowalski, B. Sieklucka, Chem. Commun. (2005) 2939–2941.
[4] L. Yi, B. Ding, B. Zhao, P. Cheng, D.Z. Liao, S.P. Yan, Z.H. Jiang, Inorg. Chem. 43 (2004) 33–43.
[5] J.M. Zheng, S.R. Batten, M. Du, Inorg. Chem. 44 (2005) 3371–3373.
[6] P.V. Bernhardt, F. Bozoglian, B.P. Macpherson, M. Martinez, Coord. Chem. Rev. 249 (2005) 1902–1916.
[7] H. Zhang, J.W. Cai, X.L. Feng, B.H. Ye, X.Y. Li, L.N. Ji, J. Chem. Soc. Dalton Trans. 11 (2000) 1687–1688.
[8] R.D. Pike, K.E. deKrafft, A.N. Ley, T.A. Tronic, Chem. Commun. (2007) 3732–3734.
[9] T.A. Tronic, K.E. Dekrafft, M.J. Lim, A.N. Ley, R.D. Pike, Inorg. Chem. 46 (2007) 8897–8912.
[10] F. Bentiss, M. Lagrenee, J. Heterocycl. Chem. 36 (1999) 1029–1032.
[11] G.M. Sheldrick, in: SHELXS-97 and SHELXL-97, University of Gottingen, Germany, 1997.
[12] C.T. Lee, W.T. Yang, R.G. Parr, Phys. Rev. B 37 (1988) 785–789.
[13] K.B. Wiberg, R.E. Stratmann, M.J. Frisch, Chem. Phys. Lett. 297 (1998) 60–64.
[14] C.C. Wang, C.H. Yang, S.M. Tseng, S.Y. Lin, T.Y. Wu, M.R. Fuh, G.H. Lee, K.T. Wong, R.T. Chen, Y.M. Cheng, P.T. Chou, Inorg. Chem. 43 (2004) 4781–4783.
[15] R. Bauernschmitt, R. Ahlrichs, F.H. Hennrich, M.M. Kappes, J. Am. Chem. Soc. 120 (1998) 5052–5059.
[16] M.D. Segall, P.J.D. Lindan, M.J. Probert, C.J. Pickard, P.J. Hasnip, S.J. Clark, M.C. Payne, J. Phys.: Condens. Matter 14 (2002) 2717–2744.
[17] J.P. Perdew, J.A. Chevary, S.H. Vosko, K.A. Jackson, M.R. Pederson, D.J. Singh, C. Fiolhais, Phys. Rev. B 46 (1992) 6671–6687.
[18] J.S. Lin, A. Qteish, M.C. Payne, V. Heine, Phys. Rev. B 47 (1993) 4174–4180.
[19] B. Delley, J. Chem. Phys. 92 (1990) 508–517.
[20] K. Nakamoto, in: Infrared and Raman Spectra of Inorganic and Coordination Compounds, 5th ed, Wiley and Sons, New York, 1997.
[21] A. Bondi, J. Phys. Chem. 68 (1964) 441.
[22] M. Du, X.J. Jiang, X.J. Zhao, H. Cai, J. Ribas, Eur. J. Inorg. Chem. (2006) 1245–1254.
[23] M. Du, Z.H. Zhang, Y.P. You, X.J. Zhao, Cryst. Eng. 10 (2008) 306–321.
[24] A.M. Kutasi, D.R. Turner, P. Jensen, B. Moubaraki, S.R. Batten, K.S. Murray, Cryst. Eng. 11 (2009) 2089–2095.
[25] A. Horvath, K.L. Stevenson, Inorg. Chim. Acta 186 (1991) 61–66.
[26] A. Horvath, K.L. Stevenson, Inorg. Chem. 32 (1993) 2225–2227.
[27] A. Horvath, C.E. Wood, K.L. Stevenson, Inorg. Chem. 33 (1994) 5351–5354.
[28] C.E.A. Palmer, D.R. Mcmillin, C. Kirmaier, D. Holten, Inorg. Chem. 26 (1987) 3167–3170.
[29] V.W.W. Yam, K.K.W. Lo, Chem. Soc. Rev. 28 (1999) 323–334.
[30] A. Horvath, Z. Zsilak, S. Papp, J. Photochem. Photobiol. A: Chem. 50 (1989) 129–139.
[31] H. Chermette, C. Pedrini, J. Chem. Phys. 75 (1981) 1869–1875.
[32] C. Pedrini, Phys. Status Solidi B 87 (1978) 273–286.
[33] M.D. Segall, P.J.D. Lindan, M.J. Probert, C.J. Pickard, P.J. Hasnip, S.J. Clark, M.C. Payne, J. Phys.: Condens. Matter 14 (2002) 2717.
[34] R. Terki, G. Bertrand, H. Aourag, Microelectr. Eng. 81 (2005) 514–523.